MODEL FOR A NOVEL CPW PHASE SHIFTER

Charles M. Jackson+, Thi Pham+, Z. Zhang*, Alfred Lee+, Claire Pettiete-Hall+

+ TRW Space and Electronics Group 90278
* Superconducting Core Technologies, Inc., Golden CO 80401

Abstract

A multilayer CPW phase shifter combining high temperature superconductor and ferroelectric thin films produces 150 degrees of phase shift per cm at 10 GHz with a 30 Volt bias at 60 K. A quasistatic model for the effective dielectric constant and loss tangent is presented and compared with data and commercial software.

Introduction

The combination of high temperature superconductor (HTS) and ferroelectric thin film materials offers a new approach to microwave phase control devices [1,2]. Ferroelectric materials provide a variable dielectric constant for phase shifter applications [3,4,5], but progress has been limited by lack of a suitable combination of materials and high losses [6]. Fortunately, using new low loss dielectric materials and HTS films that have become available in recent years, phase shifters can be fabricated because the lattice parameters of the ferroelectric material $Sr_xBa_{1-x}TiO_3$ matches the high temperature superconductor $YBa_2Cu_3O_7$. Other recent ferroelectric phase shifters that take advantages of new materials to achieve phase shifts [7-9].

To take advantage of these new materials in a thin film geometry, design tools must be proven. This short note demonstrates that a quasistatic analysis [10] of the multilayer CPW structure is sufficient to enable circuit design by comparison to commercial simulation software, and by comparison to measured data.

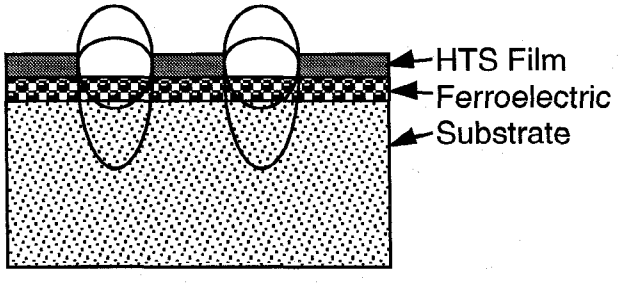

Figure 1. Coplanar waveguide CPW geometry, with ferroelectric layer under the HTS film.

This modeling paper shows the range of validity for the quasistatic analysis; a spectral domain approach is only required near the superconducting transition, or for large structures. The effective loss tangent can be obtained by this model; predicting the loss of a ferroelectric device will be an important design parameter for practical devices.

Circuit Description

Figure 1 shows a cross section of the HTS/ ferroelectric structure tested in for this paper. The results are qualitatively similar to the case where the ferroelectric film is on top of the metallization.

A filling factor method is used to calculate the impedance, effective dielectric constant, and effective loss tangent of a multilayer CPW geometry. The quasistatic model is easily programmable, and it is suitable for an initial analysis of the geometry. The equations for the filling factors of the quasistatic calculation based on a conformal mapping analysis [10] are given below.

$$k_{i1} = \frac{\sinh(\frac{\pi}{4} \bullet \frac{s}{h_i})}{\sinh\left[\frac{\pi}{4h_i}(s+2W_1)\right]}$$

where s is the center line width, W_1 is the gap width, and h_i is the layer thickness

To calculate the filling factor, we define $k = k_{N+1} = k_{M+1}$. The filling factor is given by

$$q_i = \frac{K'(k)}{2K(k)} \bullet \left[\frac{K(k_i)}{K'(k_i)} - \frac{K(k_{i-1})}{K'(k_{i-1})}\right]$$

For the multilayer structure considered here, an effective real part of the dielectric constant can be redefined, by a re-indexing of the layers:

TH 3F

CH3577-4/95/0000-1439$01.00 © 1995 IEEE

$$\varepsilon'_{eff} = \sum_{i=1}^{n} q_i \varepsilon'_i$$

Where q_i is the filling factor, and the subscript refers to the layer of the CPW structure. Similarly, an effective complex part can be defined:

$$\varepsilon''_{eff} = \sum_{i=1}^{n} q_i \varepsilon''_i = \sum_{i=1}^{n} q_i \varepsilon'_i \tan\delta_i$$

With these equations, an effective loss tangent can be defined as the ratio of the effective real and imaginary parts of the dielectric constant:

$$\tan\delta_{eff} = \frac{q_1\varepsilon_1 \tan\delta_1 + q_2\varepsilon_2 \tan\delta_2}{q_1\varepsilon_1 + q_2\varepsilon_2 + q_3\varepsilon_3}$$

where we have taken $\tan\delta_3 = 0$ for the layer of air above the ferroelectric film. The attenuation constant of a transmission line is given by [11]:

$$\alpha = \frac{27.3}{Q_o \lambda_m}(dB/cm) \quad \text{where } \lambda_m = \lambda_0/(\varepsilon_{re})^{1/2}$$

For the case of microstrip and CPW [11], for this multilayer geometry, using the effective loss tangent definition, the expression is:

$$\alpha = 0.91\sqrt{\varepsilon_{eff}}F(GHz)\tan\delta_{eff}(dB/cm)$$

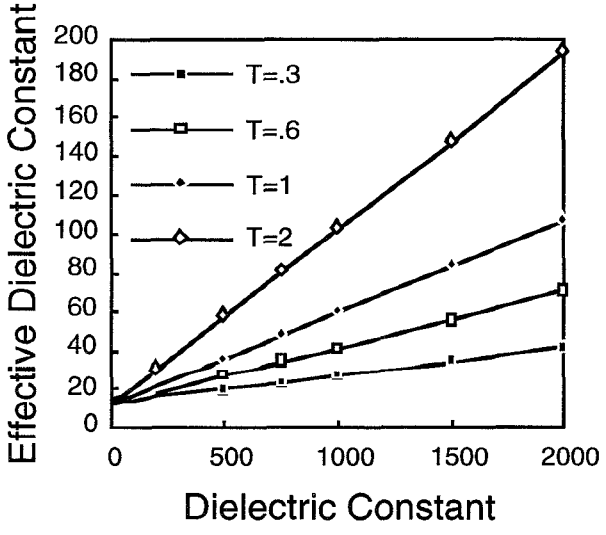

Figure 2. Relation of dielectric constant on effective dielectric constant for S=10 and W=19 μm.

For a CPW geometry, a series of plots can be generated for the total attenuation for a 1 cm line at 10 GHz. Fig. 2 shows effective dielectric constant for different ferroelectric film thicknesses, and Fig. 3 shows the attenuation values for different real parts of the dielectric constant, for different values of the film loss tangent, for a 0.3 μm thick film, on a 508 μm $LaAlO_3$ substrate.

Calculations show that the impedance decreases with increasing film thickness and buffer dielectric constant. The effect is smaller for larger gaps. The plot, Fig. 2, shows the change in the effective dielectric constant with buffer dielectric constant for four buffer thicknesses. The effect for thick films with high dielectric constants can be large.

Figure 3 shows the attenuation versus film dielectric constants for different film loss tangents. The thicker films cause higher attenuations.

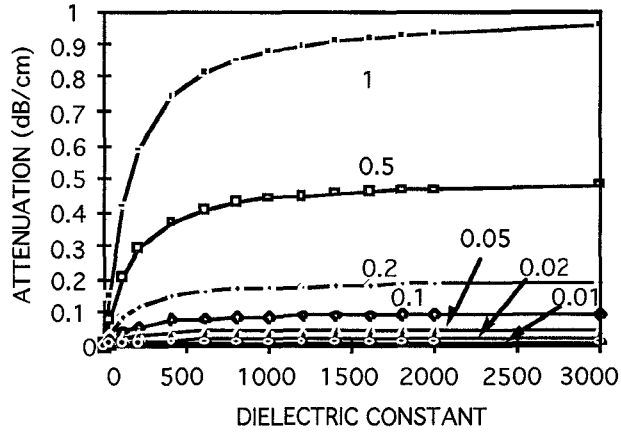

Figure 3. Plot of effective loss tangent versus film dielectric constants for different film loss tangents. For s=10 μm, w=19 μm, and t=2.0 μm. Based on a quasistatic calculation

A comparison of the effective dielectric constants (Fig. 4) and the effective loss tangents (Fig. 5) as calculated by SONNET and the quasistatic model shows that the quasistatic model is surprisingly accurate.

The quasistatic model and the SONNET model give good agreement on the value of the effective dielectric constant (Fig. 4) and reasonable agreement for the effective loss tangent (Fig. 5). The effective dielectric constant is smaller for larger gaps, and the loss is smaller for larger gaps, thinner films, and lower loss films.

As the thickness of the film increases, the effective dielectric constant increases, but the increase is less than linear for thicker films. The close agreement of the two calculations shows that it is possible to use the quasistatic technique to predict the dielectric constant and impedances.

A calculation of the frequency dependence of the effective loss tangent as calculated by SONNET shows

small variations up to 20 GHz. The slight frequency dependence may be due to the chosen length of line, or the cell size.

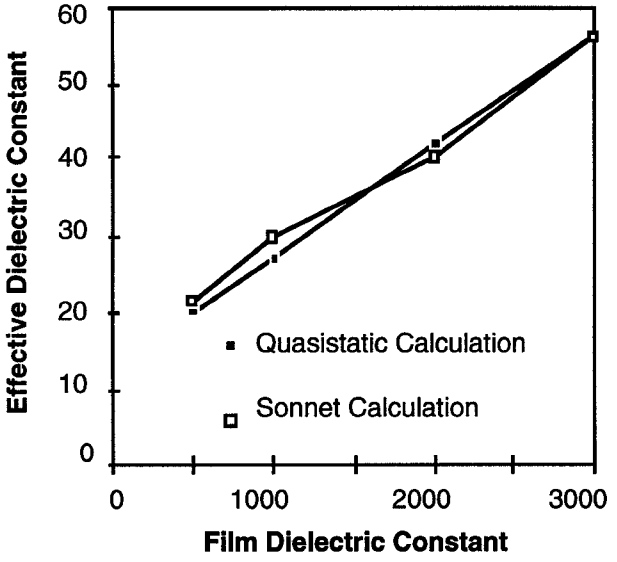

Figure 4. Comparison of SONNET and quasistatic models. Plot of effective dielectric constant ε' versus film dielectric constants that is independent of film loss tangents. The SONNET calculation (open squares) is at 20 GHz for s=10 μm, w=19 μm, and t=0.3 μm.

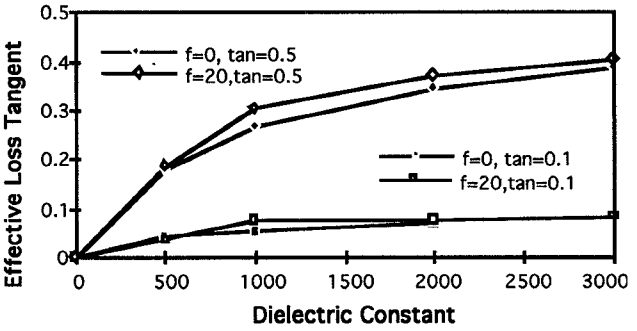

Figure 5. Comparison of SONNET and quasistatic models. Plot of effective loss tangent versus film dielectric constants for different film loss tangents calculated by a quasistatic model and by SONNET at 20 GHz for s=10 μm, w=19 μm, and t=0.3 μm.

Experimental verification of the model is difficult because it is not possible to deposit thin films of arbitrary dielectric constants, so a comparison of theory and measurement depends on the comparison of two measurements of the dielectric constant of the film. Furthermore, low frequency data may not extrapolate to high frequency data. Comparison of the theory to loss tangent data is very difficult because no independent method for determining the loss tangent is possible.

Measurement of an interdigitated capacitor determined the dc capacitance of the films. Based on the geometry of the structure [12] and the capacitance data in Fig. 6, the low frequency maximum dielectric constant was 5640. Measurements of the phase changes on a 0.55 cm CPW line, Fig. 7, line determined a maximum value of 5070. The differences between the two numbers are most likely due to calibration issues at 10 GHz. The insertion loss and phase change of a 0.55 cm line are shown in Fig. 8. Comparison of Figures 8 and 9 shows that the insertion loss is dominated by the ferroelectric film. The onset of the superconducting kinetic inductance effect appears near the superconducting transition, around 90 K. Near the superconducting transition, a better model is needed; for devices using normal metals, this quasistatic model should suffice. Fig. 9 shows the 10 GHz thin film dielectric constant measurements determined from the data of Fig. 7.

ε	DC Figure 6	CPW (10 GHz) Figure 9
Peak at 0 V	5640	5071
Peak at 30 V	1275	2765

Table 1. Comparison of the calculated dielectric constants of a $SrTiO_3$ film at the zero bias peak at 80 K.

Conclusion

This short note has described a broadband CPW phase shifter combining the low loss of high temperature superconductors and the variable dielectric constant of ferroelectrics is described. A phase shift of 140 degrees at 10 GHz with a 30 V bias has been demonstrated at 65 K. A quasistatic filling factor model has been compared to more sophisticated techniques with excellent agreement. The phase shifter shows low insertion loss, and uniform time delay between 2 and 18 GHz [4]. A more complex model is needed near the superconducting transition, but for normal metals or below the superconducting transition, this quasistatic model will provide the necessary information.

Acknowledgments

This work was supported by contract N00014-91-C-0199.

References

1. Satyen Das, "HTS Ferroelectrics Form High-Power Pase Shifters", Microwaves and RF, 137-144 (December 1994)
2. O. Vendik and L. Ter-Martirosoyan, "Superconductors Spur Application of Ferroelectric Films", Microwaves and RF, 67-70 (July 1994)
3. S.V. Orlov, A.D. Levin, and L.I. Kiseleva, "Characteristics of Ferroelectric Microwave Phase-

Shifters", Izvestiya VUZ. Radioelektronika, Vol. 27, No. 11, pp 83-85, 1984
4. A. Kain, T. Pham, C. Pettiette-Hall, A. Lee, Z. Zhang, M. Heiney, R. Yandrofsky, and C.M. Jackson, "Broad-band Phase Shifter Combining High Temperature Super-conductors and Ferroelectric Thin Films", presented at the 5th International Conference on Integrated Ferro-electrics (March 1994)
5. D.C. Degroot, J.A. Beall, R.B. Marks, and D.A. Rudman, "Tunable Microwave Properties of YBa2Cu3))7-d/SrTiO3 Thin Film Transmission Lines", presented at the Applied Superconductivity Conference (October 1994)
6. V.K. Varadan, D.K. Ghodgaonkar, V.V. Varadan, J.F. Kelly, and P. Glikerdas, "Ceramic Phase Shifters for Electronically Steerable Antenna Systems", Microwave Journal Vol. 35, No. 1 Jan. 1992.
7. R. Wolfson and B. Pierce, "An X-Band Ferroelectric Phase Shifter", to be published
8. K.R. Carroll, J.M. Pond, D.B. Chrisey, J.S. Horwitz, R.E. Leuchtner, and K.S. Grabowski, "Microwave measurements of the dielectric Constant of $Sr_{0.5}Ba_{0.5}TiO_3$ ferroelectric Thin Films", Applied Physics Letters, 62, 1845-1857 (1993)
9. J.A. Beall, R.H. Ono, D. Galt, and J.C. Price, "Tunable High Temperature Superconductor Microstrip Resonators", 1993 MTT Symposium Digest., pg 1421-1423 (1993)
10. J. Svacina, "A Simple Quasi-static Determination of Basic Parameters of Multilayer Microstrip and Coplanar Waveguide", IEEE Microwave and Guided Wave Letters, Vol. 2, pp 385-387 (1992)
11. K.C. Gupta, R. Garg, I.J. Bahl, Microstrip Lines and Slotlines, Artech House, inc., Dedham MA, 1979
12. H-D. Wu, Z. Zhang, F. Barnes, C.M. Jackson, A.Z. Kain, and J. Cuchiaro, "Voltage Tunable Capacitors Using HTS and Ferroelectrics", IEEE Applied Superconductivity vol. 4, 156-160 (1994)

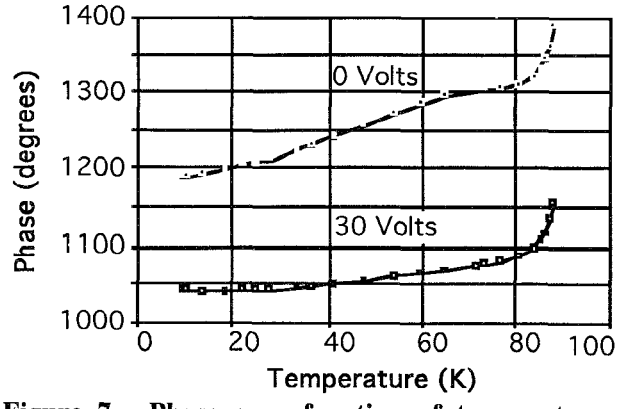

Figure 7. Phase as a function of temperature, referenced to an calibration line. The increase near 90 K is due to the kinetic inductance effect.

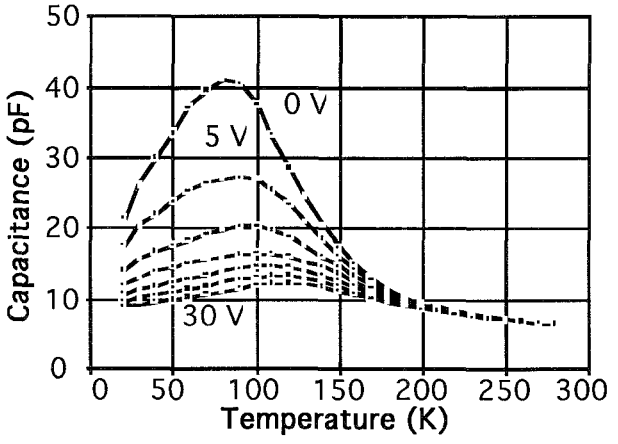

Figure 6. Interdigitated capacitor data. An interdigitated capacitor with 40 fingers, a gap of 15 μm, a width of 10 μm, thickness of 0.6 μm, and a length of 508 μm, on a $LaAlO_3$ substrate, measured between 0 and 30 V in 5 V steps.

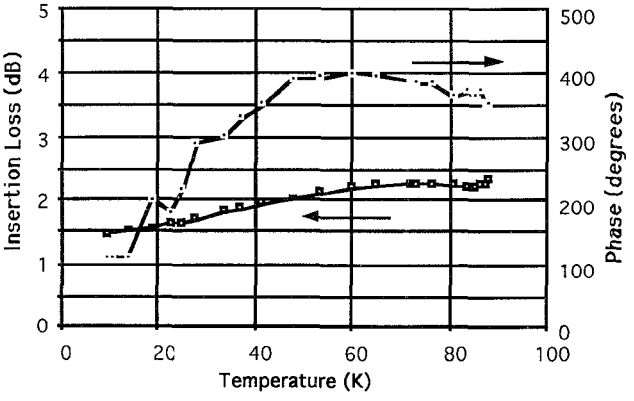

Figure 8. Insertion loss and phase shift as a function of temperature for the $SrTiO_3$ film with dc data in Figure 6.

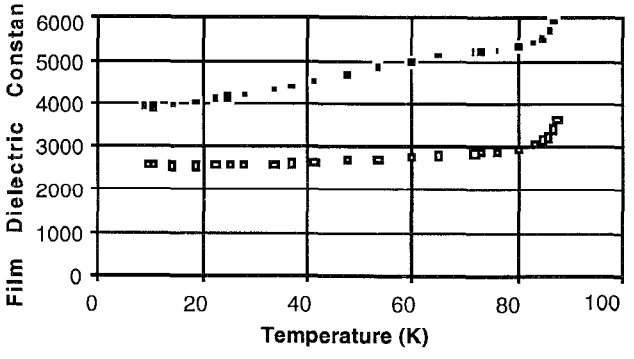

Figure 9. Film dielectric constant determined from CPW measurements at 10 GHz. Peak values are summarized in Table 1